EVOLUTION OF THE MICROSTRUCTURE AND MAGNETIC PROPERTIES OF MELT SPUN Fe_2NiAl ALLOY DURING AGING

MENUSHENKOV Vladimir, GORSHENKOV Mikhail, SHCHETININ Igor, SAVCHENKO Elena

National University of Science and Technology "MISiS", Moscow, Russian Federation,
menushenkov@gmail.com

Abstract

A microcrystalline Alni alloy with the nominal composition $Fe_{51.1}Ni_{23.5}Al_{23.7}Si_{1.7}$ was prepared by melt-spinning. Detailed studies of the spinodal decomposition (SD), microstructure and magnetic properties of the ribbons subjected to isothermal aging at T_{ag} = 500-780 °C are reported. TEM investigations of the decomposition of the solid solution ($\beta_2 \rightarrow \beta + \beta_2$) after melt-spinning and aging have revealed several types of decomposition products. As prepared melt spun ribbons show zone structure and antiphase domain (APD) boundaries inside grains. Aging at 500-600 °C led to the coarsening of the zone microstructure and to the appearance of discontinuous precipitates (DP) ($\beta + \beta_2 \rightarrow \beta' + \beta'_2$) at grain boundaries. Aging at higher than 650 °C causes the formation of a modulated microstructure instead of a zone microstructure inside grains and coarsening of DP products. As prepared ribbons reveal soft magnetic properties (H_c = 480 $A \cdot m^{-1}$). The maximum coercivity H_c = 20 $kA \cdot m^{-1}$ was obtained for the ribbons aged at 700 °C. MFM method was used to image the magnetic microstructure of melt spun Alni ribbons subjected to aging.

Keywords: Alni alloy, melt-spinning, aging, antiphase domains, discontinuous precipitates

1. INTRODUCTION

Hard magnetic materials based on Fe-Ni-Al alloys have high coercivity value arising due to spinodal decomposition (SD) of the solid solution ($\beta_2 \rightarrow \beta + \beta_2$). Recent studies of Alni and Alnico alloys [1-8] gave new results which show that magnetic properties of these alloys could be further improved. The properties of melt spun FeNiAl-based ribbons distinct from those of as-cast alloys. The microstructure, as well as the magnetic properties of the ribbons, are largely determined by the cooling rate used to solidify from the melt and temperatures of subsequent aging [5-8]. The grain boundaries (GB) and antiphase domain (APD) boundaries are markedly affected by the SD products. A discontinuous precipitation (DP) has been observed in the Fe_2NiAl ribbons after subsequent aging. The cellular microstructure at GBs consisting of alternating lamellas of β'- and β'_2 phases was sighted after aging the ribbons at 500 °C [6]. The effect of GB on spinodal decomposition leading to the formation of DP at the GB has been studied using computer simulation [9-11]. Despite above structural progress, the influence of the SD products on coercivity in melt spun Alni alloys is not clear yet. In this study, the microstructure and magnetic properties have been investigated in the melt spun Alni alloy after aging at different temperatures. The peculiarities of the spinodal decomposition on the GBs and APD boundaries and the DP reaction development at the GBs during the aging of melt spun ribbons at the temperatures 500-780 °C are reported.

2. EXPERIMENTAL PROCEDURE

The Alni alloy of the nominal composition $Fe_{51.1}Ni_{23.5}Al_{23.7}Si_{1.7}$ was studied. The cast ingot was melted and quenched by melt-spinning with a copper-wheel speed v ~ 40 $m \cdot s^{-1}$. The thickness of the melt spun ribbons was 20-40 μm. The aging of ribbons was carried out in an argon atmosphere at 500-780 °C for 10 min. The structures of the samples were examined by TEM using a JEM-1400 microscope operated at 120 kV. The thin foils for TEM were prepared by electro-polishing a Struers TenuPol 5 jet polisher. The ribbon micro-relief was

studied by atomic force microscopy (AFM) of AIST-NT manufacturer in a taping mode. Magnetic force microscope (MFM) was employed to image the magnetic domain structure in the ribbons with a typical lift height of 50 nm and a high moment Co-coated tip magnetized normally to the sample surface. The magnetic properties of the ribbons were measured at room temperature using a PPMS EverCool-II (Quantum Design) magnetometer.

3. RESULTS AND DISCUSSION

Fig. 1 shows (*a*) bright- and (*b*) dark-field images of the microstructure of Alni ribbon quenched from the melt and (1b, inset) associated electron diffraction pattern taken in 001 superlattice reflection. As-prepared ribbons have soft magnetic properties (H_c = 478 A·m^{-1}). In accordance with [6], the microstructure of Alni ribbon conforms to the zone structure which was formed due to partial decomposition of solid solution into β and β_2 phases. The twisted lines correspond to positions of APD boundaries, which are decorated by precipitates of decomposition products. The antiphase domains are also observed in 001 reflection (**Fig. 1b**) because the electron phase shift is not zero (displacement vector for APD in B2 is a/2<111>). The sequential ordering took place during the spinning of the alloy and APDs were formed during solidification from the melt via nucleation and growth mechanism (transformation of disordered A2 to ordered B2) [6].

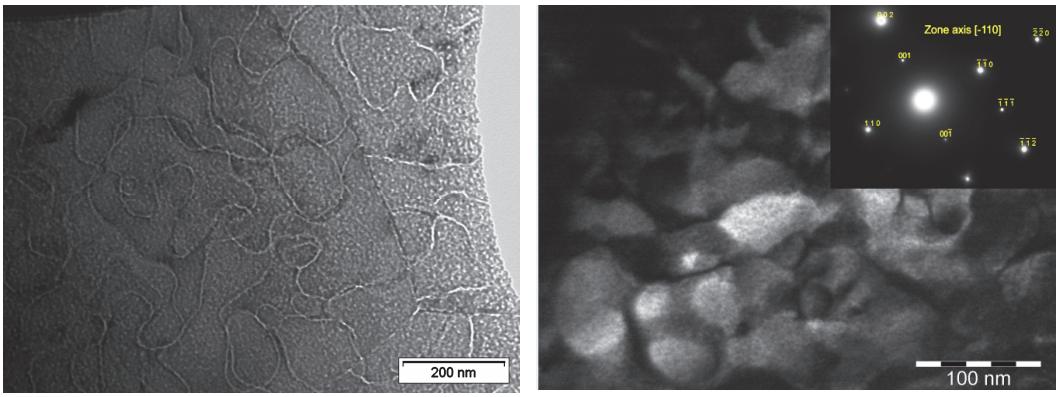

Fig. 1 Bright-field TEM micrograph of Alni ribbon and (b) darkfield image taken in 001 reflection and subsequent diffraction pattern (inset)

Fig. 2 shows TEM micrographs of the microstructure of the melt spun ribbons aged at 500, 550 and 600 °C (for 10 min), respectively. The ribbons aged at 500-600 °C demonstrated low coercive force comparable with as-prepared ribbons. For example, aging at 600 °C for 10 minutes increases H_c only up to 5 kA·m^{-1}.

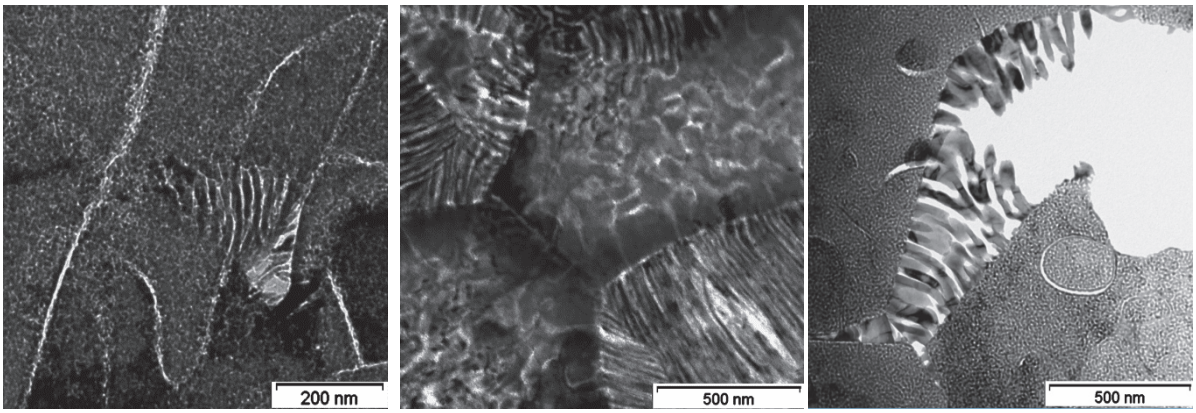

a) b) c)

Fig. 2 Bright-field TEM micrograph of the ribbons aged at 500, 550 and 600 °C for 10 min

The aging led to the coarsening of zone microstructure inside the grains (normal SD) and to the appearance of discontinuous precipitate (DP) at GBs. The DP in the form of alternating lamellas of the β' and β'_2 phases were grown from GBs with lamellar spacing approximately 20 nm. It may be assumed, that DP is formed by reaction $\beta + \beta_2 \rightarrow \beta' + \beta'_2$, where $\beta + \beta_2$ is initial SD structure within grains [5-8]. The lamellas were oriented not only in the ribbon plane but also perpendicular to it in a random way.

Fig. 3 shows micrographs of the microstructure of the ribbons aged at 700 and 780 °C for 10 min, respectively. As is seen in these pictures, there are several types of structural components in the microstructure of the ribbons aged at 700-780 °C; these are the modulated structure within grains, alternating lamellas between some grains, and intergranular double-layers of the phases formed by the coarsening and transformation of the initial DP product.

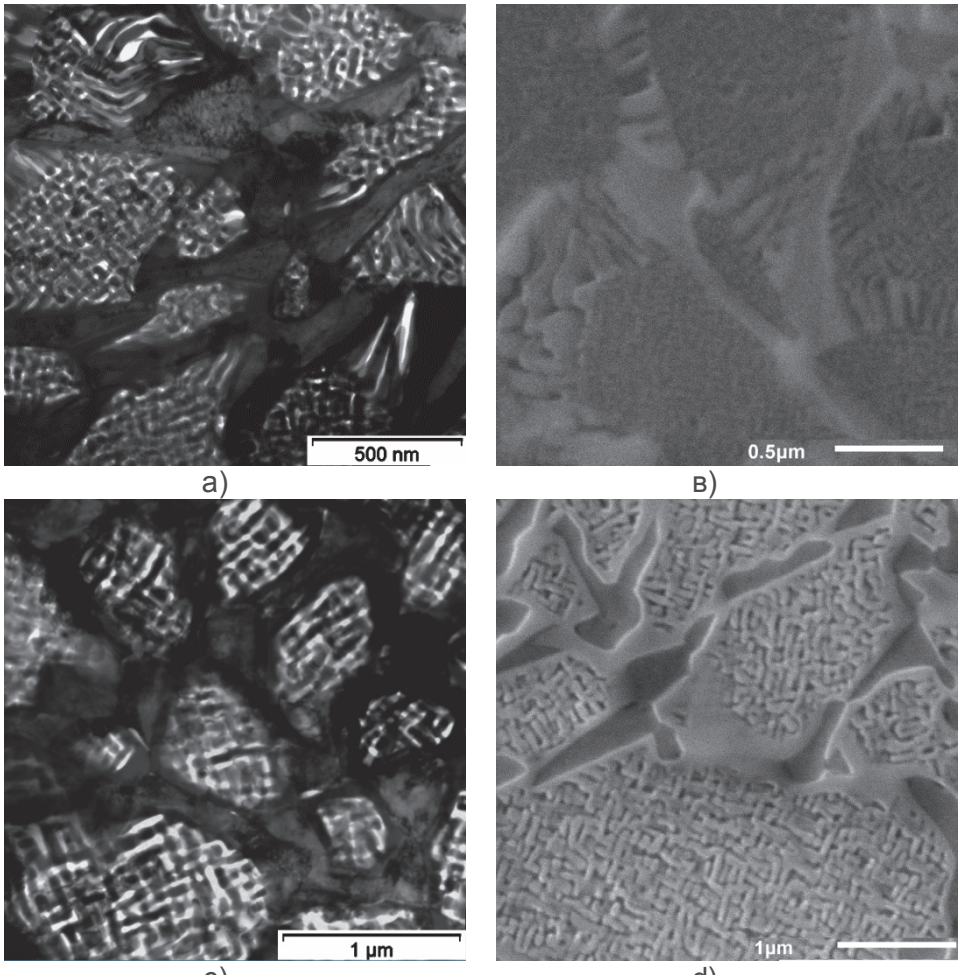

Fig. 3 (a,c) Bright-field TEM micrograph and (b,d) SEM image of the ribbon aged at 700 and 780 °C

The aging at 700 °C for 10 min led to the formation of a modulated microstructure (normal SD) inside the grains with the wave length of approximately 100 nm (**Fig. 3a, b**). The coercive force of this sample was 20 $kA \cdot m^{-1}$, which is the highest value for aged ribbons. The coarsening and particular coalescence of DP were founded at grains boundaries after the aging. The lamellar spacing of DP was 50 nm in thickness and 200-300 nm in length.

The bright-field TEM micrograph and SEM image of the ribbon aged at 780 °C is shown on **Fig. 3c, d**. Since the increase in aging temperature lead to the depth decomposition of solid solution. The increase in temperature of aging leads to coalescence of β'- and β'_2 lamellas and the formation of surrounding cores made

of β'_2- phases inset in almost continuous net of β' phase. After aging at 780 °C for 10 min, the size of the β and β_2 precipitates of modulated microstructure inside the grains increased up to 150-300 nm. The H_c of the Alni ribbons aged at 780 °C decreased up to 10 kA·m^{-1} which may be the result of the coarsening of magnetic β particles of the modulated microstructure inside the grains along with continuous β' net. After aging at 700 °C, the modulated structure consists of β- and β_2 phase particles some of which are arranged predominantly along the crystalline axis, but after aging at 780 °C, the elongated particles are arranged mainly along <100> cubic directions.

Fig. 4 a shows the temperature dependence $H_c(T_{ag})$ and the hysteresis loops for the as-prepared ribbon and the ribbons aged at 550 and 700 °C for 10 min. The as-prepared ribbons exhibit soft magnetic properties (H_c = 1.27 kA·m^{-1}).The increase in coercivity was observed as the aging temperature increases above T_{ag} > 600 °C. The maximum H_c = 20 kA·m^{-1} was obtained after aging at T_{ag} = 700 °C for 10 min.

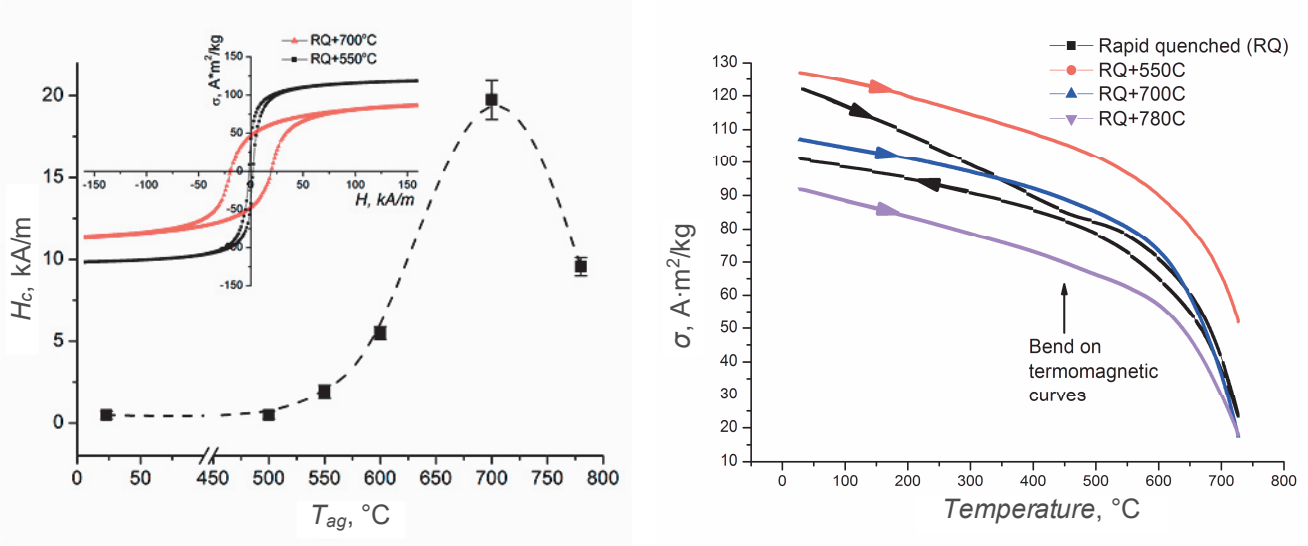

Fig. 4 Temperature dependence $H_c(T_{ag})$ and the hysteresis loops (inset), (*b*) TMA curves curve of as-prepared ribbons and the ribbons aged at 550, 700 and 780 °C

Fig. 4b shows the temperature dependence of σ measured in H = 2.39 kA·m^{-1} of the as-prepared ribbon and the ribbons aged at 550, 700 and 780 °C. The $\sigma(T)$ curve of as-prepared ribbon shows the bend at around 455 °C. After aging the ribbons at T_{ag} = 600-700 °C the bend cannot be found. But after aging at 780 °C the little bend appears again at around 470 °C. It may be assumed, that during melt spinning the zone structure is formed, wherein the compositions of the β- and β_2 phases are separated until the values corresponding to the composition of these phases at temperature about 800 °C. Hence a paramagnetic state of β_2 phase in the melt spun sample can be concluded. Therefore, during subsequent heating by TMA the bend on the $\sigma(T)$ dependence shows the start of the DP reaction and formation of the $\beta' + \beta'_2$ lamellar structure. Note that all $\sigma(T)$ curves in **Fig. 4b** show that during cooling to RT the magnetization of the samples becomes lower than during heating.

For understanding the magnetization mechanism, the magnetic domain structure in the ribbons was investigated. **Fig. 5** shows (*a*) topographic and (*b*) magnetic force images of the ribbon aged at 780 °C observed using AFM and MFM, subsequently. The wide intergranular layer of ferromagnetic β phase and modulated structure inside grains are observed in the topographic image. The corresponding magnetic force image is characterized by brighter areas which are located exactly at the site of the β phase layers and the mixture of the bright and darker areas of sub-micron scale inside the grains which correspond to the β phase precipitates into modulated microstructure. The bright areas in **Fig. 5b** indicate that the magnetization direction in the soft magnetic phase is nearly parallel to the upward tip magnetization, and the dark areas indicate the

opposite. The magnetic force image clearly shows that the size and form of the magnetic domains is same as the magnetic β phase network and the β phase particles in modulated microstructure (**Fig. 5a**).

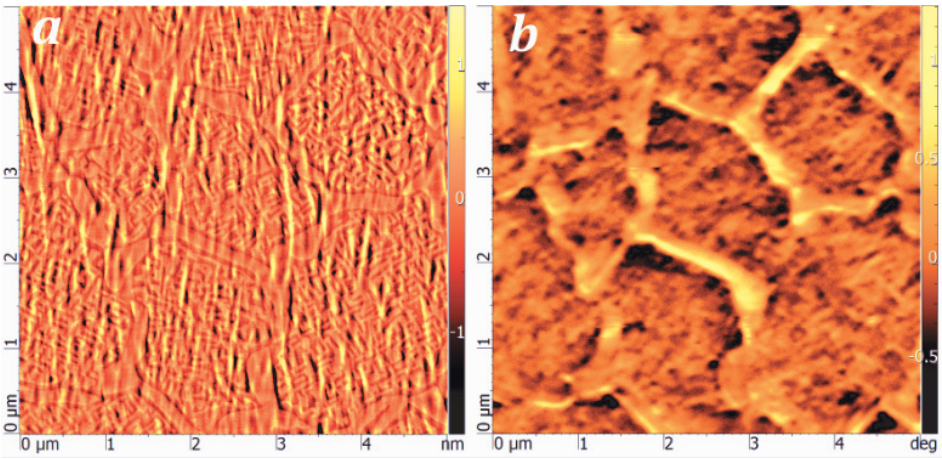

Fig. 5 (a) AFM and (b) MFM images of the ribbon aged at 780 °C for 10 min

4. CONCLUSIONS

TEM investigations of the spinodal decomposition of the solid solution ($\beta_2 \rightarrow \beta + \beta_2$) in melt spun AlNi ribbons subjected to aging have revealed several types of evolution of decomposition products. Firstly, normal SD led to the formation of zone structure inside grains and decorating of the APD boundaries with SD products. Secondly, aging at 500-600 °C of the ribbons resulted in the formation of a DP reaction at GBs, which forms the lamellar microstructure consisting of alternating lamellas of β' and β'_2 phases. Thirdly, the development of DP and SD at the higher temperatures led to β'- phase core formation inset in continuous net of β'_2 phase. Fourthly, the periodic modulated structure inside grains is formed after aging of the ribbons at a temperature higher than 700 °C, which ensures the coercive force up to H_c = 20 kA·m^{-1}. The aging of ribbons at 780 °C decreases coercive force to H_c = 9.5 kA·m^{-1} which are caused by β particles coarsening along with formation β' continuous net. Hence, peculiarities of the structure transformations and formation of the several types of evolution of decomposition products side by side with the periodic modulated structure lead to lower value of coercive force in the melt spun AlNi ribbons subjected to aging.

MFM image reflects the topographic microstructure of the ribbon surface. The domain structure is found to be complex. The coarse domains observed in the wide intergranular layer of β phase. The fine scale domains observed inside the grains indicates the magnetic domains which are formed as result of magnetic interaction between the β phase precipitates in zone or modulated microstructure.

ACKNOWLEDGEMENTS

This study was supported by the Ministry of Educations and Science of the Russian Federation, State Assignment No. 11.2616.2014/K.

REFERENCES

[1] PALASYUK A., BLOMBERG E., PROZOROV R., YUE L., KRAMER M.J., RMCCALLUM W., ANDERSON I.E., CONSTANTINIDES S. Advances in characterization of non-rare-earth permanent magnets: Exploring commercial Alnico grades 5-7 and 9. JOM, Vol. 65, No. 7, 2013, pp. 862-869.

[2] SKOMSKY R., MANCHANDA P., KUMAR P., BALAMURUGAN B., KASHYAP A., SELLMYER D.J. Predicting the future of permanent-magnet materials. IEEE Transactions on Magnetics, Vol. 49, No. 7, 2013, pp. 3215-3220.

[3] ZHOU L., MILLER M.K., PING LU, LIGIN KE, SKOMSKI R., DILLON H., XING Q., PALASYUK F., MCCARTNEY M.R., SMITH D.J., CONSTANTINIDES S., MCCALLUM R.W., ANTROPOV V., KRAMER M.J. Architecture and magnetism of Alnico. Acta Materialia, 2014, pp. 224-233.

[4] LOWE K., TABARY F., FRINCU B., MADUGUNDO R., GUTFLEISCH O., HADJIPANAYIS G. Effect of grain size on spinodal decomposition and magnetic properties of melt-spun Alnico. In Proc. of the 23rd Int. Workshop on Rare-Earth and Future of Permanent Magnets and Their Applications, Annapolis, MD, 2014, pp. 77-78.

[5] MENUSHENKOV V.P., GORSHENKOV M.V., SAVCHENKO E.S., ZHUKOV D.G. The effect of the rate of cooling from high-temperature single-phase region on the microstructure and magnetic properties of Alni alloys. Metallurgical and Materials Transactions A, Vol. 46, No. 2, 2015, pp. 656-664.

[6] MENUSHENKOV V.P., GORSHENKOV M.V., SAVCHENKO E.S., ZHUKOV D.G. Peculiarities of the spinodal decomposition and magnetic properties in melt-spun Fe_2NiAl alloyduring aging. Materials Letters, Vol. 152, 2015, pp. 68-71.

[7] MENUSHENKOV V.P., GORSHENKOV M.V., SAVCHENKO E.S. Formation of structure in an Alni alloy upon cooling from the range of single-phase solids solution and annealing. Metal Science and Heat Treatment, Vol. 56, No. 11-12, 2015, pp. 621-625.

[8] MENUSHENKOV V.P., GORSHENKOV M.V., SHCHETININ I.V., SAVCHENKO A.G., SAVCHENKO E.S., ZHUKOV D.G. Evolution of the microstructure and magnetic properties of as-cast and melt spun Fe_2NiAl alloy during aging. Journal of Magnetism and Magnetic Materials, Vol. 390, 2015, pp. 40-49.

[9] RAMANARAYAN H., ABINANDANAN T.A. Phase field study of grain boundary effects on spinodal decomposition. Acta Materialia, Vol. 51, No. 16, 2003, pp. 4761-4772.

[10] RAMANARAYAN H., ABINANDANAN T.A. Grain boundary effects on spinodal decomposition II. Discontinuous microstructures. Acta Materialia, Vol. 52, No. 4, 2004, pp. 921-930.

[11] YANG TAO, CHEN ZHENG, ZHANG JING, DONG WEI-PING, WU LIN Effect of grain boundary on spinodal decomposition using the phase field crystal method. Chinese Physics Letters, Vol. 29, No. 7, 2012, pp. 078103-1 - 078103-4.